

Assessment of Squeak and Rattle noise of a car seat using 3D sound intensity measurements

Daniel Fernandez Comesana¹, Damián Gonzalez², Tales Storani¹ and Fanyu Meng¹

¹ Microflow Technologies (NL)

² CTAG (SP)

Abstract

Squeak and Rattle (S&R) noises are transient sound events occurring when adjacent parts come into contact, either impacting or sliding. All components and sub-systems integrated in a vehicle may produce noise when excited with certain vibro-acoustic load. S&R noise can be linked to the perceived build quality, durability and even discomfort or annoyance. As a result, car manufacturers have strict regulations to prevent noise issues. Current vibro-acoustic validation tests can vary in complexity from full vehicle simulation to component level tests. Additionally, subjective assessments are often required to locate problematic areas and quantify their relevance. In this paper, S&R noise of a car seat is investigated using 3D sound intensity measurements. A multi-axial shaker is used to drive the seat with a time-stationary excitation extracted from a road profile. The impact of using different shaker configurations is evaluated. Results show that the visualization of 3D sound intensity can be used to efficiently identify the elements of a complex structure leading to S&R problems.

Introduction

The growing demand for quieter vehicles has created a new and significant challenge in the refinement process of cabin interior acoustics. The absence of sound masking effects induced by conventional powertrains exposes passengers to a variety of new noises. Especially with the advent of electric vehicles, preventing Squeak and Rattle (S&R) noise problems becomes an essential requirement.

S&R is linked to the “acoustically perceived” quality of a product commonly leading to customer complaints [1]. Previous studies have shown that S&R is the third highest reported issue amongst car buyers following powertrain and electrical problems [2]. The underlying physical mechanisms causing these phenomena are mostly related to the relative motion between two or more elements. Structural deficiencies, a poor geometrical design and/or incompatible material pairs are often found to be the root causes [3].

Most car manufacturers have developed internal methodologies and procedures to evaluate S&R [4]. Although objective tests are also performed, subjective rating is still the principal method for estimating acoustic quality. Each manufacturer has their own acceptance criteria and definitions but they are mostly based on the SAE J1060 standard [5]. The subjective evaluation is normally performed by one or more trained experts who are able to classify different noises. This method

has the advantage of being performed in-situ by experts who can detect, localize, separate and rate different noises that appear simultaneously as well as provide insight into potential solutions to the observed noises. However, reducing the inherent bias of subjective evaluation requires extensive and regular training besides panel-based assessments, where multiple experts detect and rate the unwanted noises. In addition, sharing information among development teams requires concise and detailed descriptions of the detected noises, but is difficult due to the large variety of sounds that can be observed. Therefore, an objective approach to the evaluation of S&R becomes necessary.

There is a growing trend of developing testing solutions for evaluating acoustic quality based on objective criteria. The use of measurable physical quantities in combination with well-defined signal processing algorithms has proven reliable to identify and quantify vibro-acoustic problems [6, 7].

Any acoustic field can be described by the sound pressure and particle velocity spatial variations. Three-dimensional (3D) sound intensity measurements are able to capture all available acoustic information, providing a unique starting point to solve complex problems. Furthermore, mapping the 3D sound intensity vector field enables the characterization of vibro-acoustic noise sources by evaluating the net direction of acoustic propagation (active intensity), as well as the near field interaction between closely spaced components (reactive intensity) [8].

This paper assesses the feasibility of investigating S&R problems via 3D scanning measurements of sound intensity. The impact of adjusting the excitation signal to cope with time stationarity constrains is studied. Furthermore, sound localization results of a car seat mounted on a multi-axial shaker are presented, along with a detailed analysis of each identified noise source.

Sound intensity

Sound intensity is a measure of the flow of acoustic energy in a sound field [9]. It provides not only a quantification of the acoustic emission but also the direction of sound propagation. The instantaneous sound intensity is defined as the product of sound pressure and acoustic particle velocity

$$\mathbf{I}(t) = p(t)\mathbf{u}(t). \quad (1)$$

Sound pressure and acoustic particle velocity have level and phase differences which mainly depend upon the characteristic of the sound source, measurement distance and frequency [10]. In practice it is common to study stationary sound fields in terms of the active, or propagating, part of the complex intensity averaged over time [11], i.e.

$$\mathbf{I} = [I_x, I_y, I_z] = \langle p \mathbf{u} \rangle_t = \frac{1}{2} \text{Re}\{p \mathbf{u}^*\}, \quad (2)$$

where $\langle \cdot \rangle_t$ indicates time averaging. The imaginary part of this quantity is known as the reactive intensity \mathbf{J} , which represents the non-propagating acoustic energy. Unlike the usual active intensity, the reactive intensity remains to some extent controversial probably because it has no obvious physical meaning [9]. Experimental evidence is presented in the following sections for both active and reactive intensity, discussing the practical significance of both quantities.

Figure 1 shows schematic representations of the 3D active intensity vector and the one-dimensional (1D) complex acoustic intensity, where $\theta_p - \theta_{u_n}$ represents the phase difference between the sound pressure and a particle velocity component.

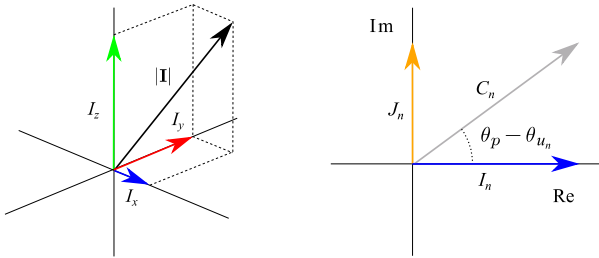


Figure 1. Schematic representation of the 3D active intensity vector (left) and 1D complex acoustic intensity (right).

Since both sound pressure and particle velocity are measured simultaneously, the calculation of the 3D acoustic intensity can be performed directly, without any approximation. This quantity provides directional information about the flow of acoustic energy. In addition, a scalar term can be extracted by taking the modulus of the active intensity vector.

Extensive research has been published exploring the fundamental differences between multiple sound intensity measurement principles and transducers [12, 13]. Pressure-based measurement methods cannot be utilized when the pressure-intensity index is high, which in practice often limits the use of p - p intensity probes in environments with high background noise or reflections. A detailed analysis of this phenomena is described in [14].

In contrast, direct intensity measurements using the combination of sound pressure and particle velocity transducers (p - u intensity probes) are unaffected by the pressure-intensity index, enabling the estimation of propagating acoustic energy despite unfavorable conditions imposed by the testing environment [12,13]. The error of intensity calculations using p - u probes mainly depends upon the reactivity of the sound field and the calibration accuracy of the probe [13]

$$\hat{I}_n \cong I_n \left(1 + \varphi_u \frac{I_n}{I_n}\right) = I_n (1 + b\{\hat{I}_n\}), \quad (3)$$

where φ_u is the phase error introduced during the calibration procedure, J_n is the reactive intensity and $b\{\cdot\}$ denotes the bias error of an estimate. If the reactivity is high, for example in the near field of a source, a small phase mismatch in the transducer's calibration may lead to considerable errors on the intensity estimates. In [14] it is stated that in practical situations the reactive intensity should not exceed the active intensity by more than 5 dB in order to achieve an accurate quantification of the active sound intensity. Although active intensity may be biased in a highly reactive field, the phase difference between pressure and particle velocity can still be measured accurately. Therefore, it is still possible to discard measurement positions which are exposed to high reactivity and ensure that the most reliable data is evaluated.

Measurement method: Scan&Paint 3D

The sound visualization system used to capture the information hereby presented was Scan&Paint 3D [8]. The system comprises the following hardware elements:

- 3D tracker: automatic real-time 3D tracking of the sensor position and orientation using a stereo infrared camera.
- Data acquisition unit: 24 bit, 4 channel data acquisition system.
- Signal conditioner: signal conditioning unit for supplying power and pre-amplification to the 3D sound intensity probe.
- 3D sound intensity probe: broadband 3D intensity probe (20 Hz to 10 kHz) consisting of a sound pressure microphone and 3 acoustic particle velocity sensors.
- Tracking sphere: open sphere with scattered IR reflecting markers for tracking the probe location and orientation.
- Remote handle: control and monitor the data acquisition process.

Before measuring the acoustic field it is required to have a 3D model of the testing object. The model can be either imported from a CAD file or obtained by scanning the area of interest with a structural scanner. Results presented below were acquired using a 3D scanner known as a structure sensor [15]. The model is used as a visual reference as well as to automatically position the 3D tracker into the measuring environment.

The acoustic data acquisition process starts by manually moving a 3D sound intensity probe whilst a stereo camera is used to extract the instantaneous position of the sensor in the 3D space.

The recorded signals are split into multiple segments and assigned to their corresponding locations using a spatial discretization algorithm [8]. The spatial resolution is defined during the post-processing stage and thus can be adjusted depending on the available data. The maximum feasible resolution is determined by the accuracy of the 3D tracker, in this case down to 3 millimeters.

A particle velocity or sound intensity vector representation of the acoustic variations across the sound field can then be computed to provide a visual representation of the sound distribution. Figure 2

shows the main hardware elements, experimental setup and analysis software.

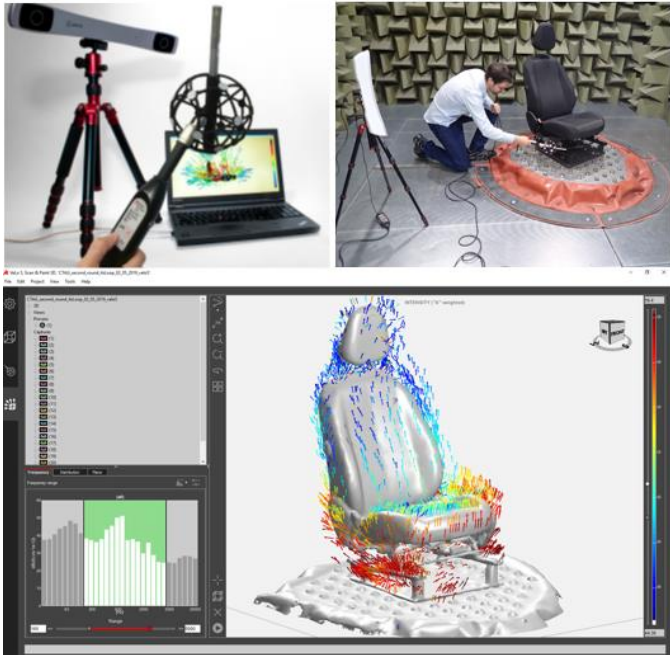


Figure 2. Scan&Paint 3D hardware (top left), experimental setup (top right) and software (bottom).

Experimental investigation

The measurement campaign evaluated in this study focuses on evaluating the S&R noise produced by a car seat from a commercial vehicle (regular production series) mounted on a shaker inside a semi-anechoic chamber. Experiments were carried at an NVH laboratory of the Automotive Technology Centre of Galicia (CTAG). The measurement data presented in this paper was captured during one single day, including preparation, data acquisition and preliminary on-site processing.

Shaker excitation

A synthetic stationary Gaussian excitation was created from a vibration signal recorded through multiple accelerometers at the base of the seat when driving on a harsh pebble stone road. The Spectral Density Matrix (SDM) of the synthetic signal was adjusted between 3 Hz and 100 Hz to match the SDM of the recorded signal, respecting both the Power Spectral Densities (PSD) and Cross-Spectral Densities (CSD). The length of the full synthesized signal was of 120 s without repetitions. Although the recorded excitation has significant energy in all six degrees-of-freedom (DOFs), different scenarios were generated in order to evaluate the impact of the number of excitation DOFs as well as the duration of the input signal on the resulting S&R noises:

- 6D: excitation with 6 DOFs (X, Y, Z, Roll, Pitch, Yaw).
- 3D: excitation with 3 DOFs (X, Y, Z).
- 1D: excitation with a single DOF (Z).
- 6D with a signal segment of 4 s repeated over 120 s.
- 3D with a signal segment of 4 s repeated over 120 s.
- 1D with a signal segment of 4 s repeated over 120 s.

All signals were played on a shaker to evaluate the worst-case seat configuration. Headrest and seat inclination were set to nominal settings, and the sliders were adjusted to full back. The duration of the repeated time signal was determined by selecting the shorter time segment that would match the subjective score using a 6D excitation.

Subjective evaluation

The unwanted noises generated by the seat when excited by the above-mentioned six signals were subjectively evaluated by multiple expert listeners. Each noise was rated for each excitation signal from 0 to 10, ranging from the most annoyance to the least, following the SAE J1060 standard [5].





Table 1 presents the results found during this investigation. It can be seen that the knocking noise produced by the headrest guides and the left slider were the primary sources of annoyance. The right slider and backrest regulation wheel were identified as secondary sources.

The severity of the problem was also dependent on the type of excitation used in the shaker, being the problematic elements more noisy when multiple degrees of freedom were used. Minor differences were perceived between 3D and 6D excitation signals, whereas 1D excitation was perceived with much less annoying.

The evaluation of the complete signal or the repeated short segment yielded very similar subjective scores. This is likely to be due to the fact that the synthesized signal is Gaussian and Wide-Sense Stationarity (WSS). Since the statistical characteristics will not significantly vary over time, a 4 s section of the 120 s signal will basically retain all the statistical properties of the larger signal. This will probably not occur if a recorded time history is used.

These results support the assumption that data obtained via scanning measurements could be directly correlated with the noise perceived in the 120 s test.

Table 1. Scores of the subjective evaluation performed with several types of excitation. NND refers to no noise detected.

#	Photo	Description	120 s			Repeated 4s		
			6D	3D	1D	6D	3D	1D
1		Knocking of headrest guides against their guideways in upper position	5	5	7	5	5	7
2		Knocking in left slider. Contact between upper and lower profile	6	7	8	6	7	8
3		Knocking in right slider. Contact between upper and lower profile	7	8	8	7	7	8
4		Knocking of the backrest regulation wheel	7	7	NND	NND	NND	NND

Scanning measurements

Multiple measurements were performed around a car seat, aiming to achieve high spatial resolution sound mapping. A total of 22 scans adding up to approximately 45 minutes were captured using a Scan&Paint 3D system. The tracking camera was set in two locations to capture a full view of the seat. A picture of the setup along with a preview of the scanned structure highlighting the scanning traces with different colors is shown in Figure 3.

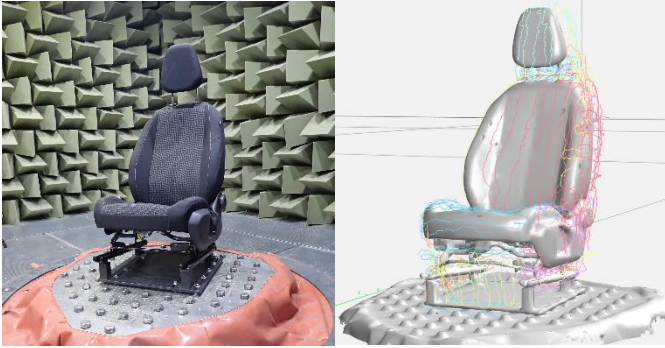


Figure 3. Picture of the evaluated car seat with the worst-case configuration (left) and a preview of the 22 scanning traces (right).

This work focuses on studying the regime of excitation leading to the highest annoyance, i.e. when the shaker is excited with 6 DOFs. The signal segment of 4 s repeated over 120 s was chosen to ensure that stationarity would be preserved during the scanning tests.

3D sound intensity visualization

The large dataset acquired contains information about the spatial distribution of sound pressure, particle velocity and (active & reactive) sound intensity around the testing object in full 3D space. This section shows some of the main findings, but it should be noted that more in-depth analysis could be performed around any particular area or any frequency band of interest.

Figure 4 shows the broadband 3D sound intensity mapping (20 Hz to 10 kHz) along with the spatially averaged power spectrum. The vector field indicates that the bottom section of the seat and shaker plate are the main noise sources in the low and mid frequencies, which is in agreement with the frequency range of the excitation signal used to drive the shaker.

It should be considered that this result combines the sound radiated by the seat due to S&R as well as the background noise produced by the shaker. Therefore, a detailed analysis of each of the noise sources requires selecting appropriate frequency limits.

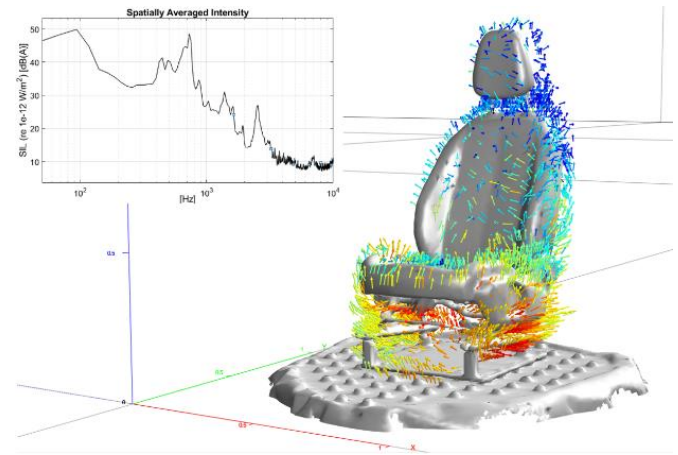


Figure 4. Overall sound intensity mapping (20 Hz to 10 kHz) with a 20 dB dynamic range.

Computing visualization results considering the statistical distribution of the measurements is key to filter and avoid irrelevant data. This filtering process becomes particularly useful for S&R problems when the temporal variability is high in a short time scale. The histogram of the sound intensity levels was used to constrain the data by setting level limits. Figure 5 shows the results with and without histogram filtering. As shown, the location of the main problematic areas becomes clear when 50% of the data containing the lowest levels is hidden.

In this particular case, noise events around the headrest area were produced every few seconds, so there are certain measurement grid cells which do not contain information related to S&R. Therefore, constraining the histogram helps to display the most relevant data for noise localization.

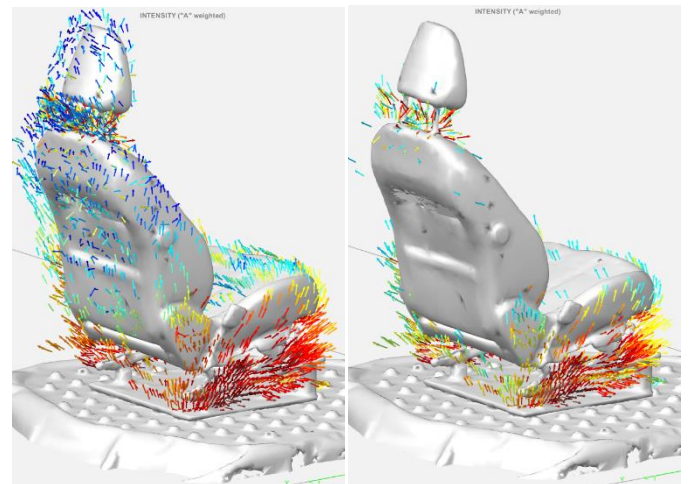


Figure 5. High frequency sound intensity mapping (800 Hz to 10 kHz) for all data (left) and hiding 50% of the data point with low levels (right) with a 15 dB dynamic range.

In addition, Figure 6 shows the spatially averaged sound intensity spectra around the main elements of interest. This preliminary analysis shows that the headrest and seat sliders are the main noise contributors besides the shaker plate.

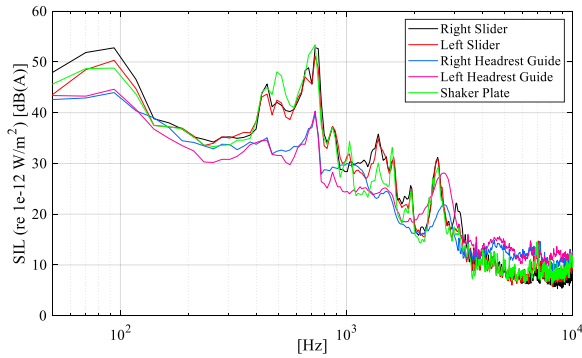


Figure 6. Spatially averaged sound intensity around the main elements of interest, highlighting their excitation per frequency band.

The following subsections are focused on providing further insight on the main noise sources highlighted.

Headrest

The headrest was identified as one of the main problematic areas. As a result, additional analysis was performed on this area of interest. Firstly, a spatial filter was applied to exclude all data outside the control volume.

Secondly, third octave mapping results were evaluated but for the sake of brevity they were excluded from this publication. A consistent pattern was found within two frequency ranges displayed in Figure 7.

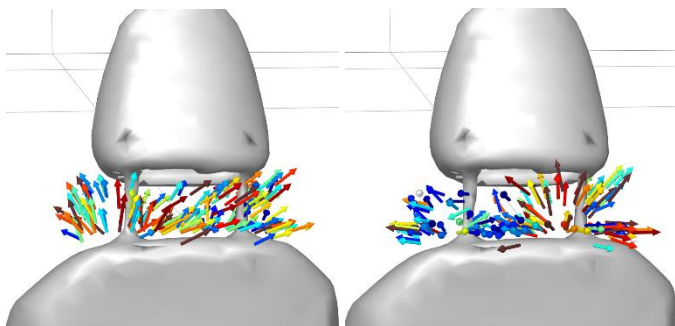


Figure 7. Sound distribution of the headrest area in two frequency ranges: 800 Hz to 2 kHz (left) and 2 kHz to 10 kHz (right) with 12 dB dynamic range.

The connections between both headrest guides and guideways seem to be the primary sources of S&R, which is in line with the subjective evaluation. Furthermore, it can be concluded that the right guide of the headrest is the dominant source of noise in the range between 800 Hz and 2 kHz, whereas the left guide is dominant above 2 kHz. The convention for denoting “left” and “right” was the same as during the subjective evaluation, i.e. opposite to what a person seating on the car seat would use.

Although the level fluctuations between contiguous arrows are to some extent large, the direction of propagation remains consistent and smoothly changing over space. The locations of the main sources generating the sound field can be estimated by following the arrows in opposite direction to their propagation, converging towards the origin points.

Seat sliders

The other problematic elements identified in Figure 5 were the seat sliders connecting the seat structure and the bottom frame that is attached to the vehicle floor (or in this case the shaker plate). Figure 8 shows a comparison of both sides in the same frequency ranges as in the last subsection (800 Hz to 2 kHz and 2 kHz to 10 kHz). As illustrated, there is significant sound radiation along the slider frames from both sides.

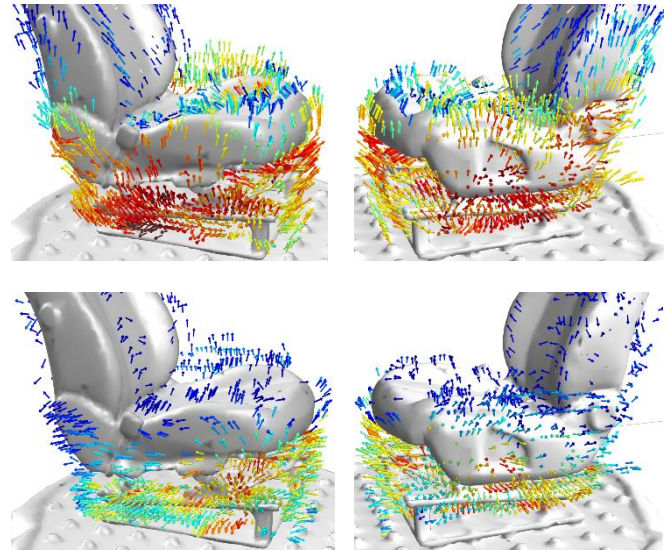


Figure 8. Sound distribution of the left and right sliders in two frequency ranges: 800 Hz to 2 kHz (bottom) and 2 kHz to 10 kHz (top) with a 15 dB dynamic range.

The high density of arrows in 3D space may cause difficulties interpreting the results and localizing the noise sources. Figure 9 shows additional sound visualization results constrained to 2D slices centered at the seat sliders and headrest guides.

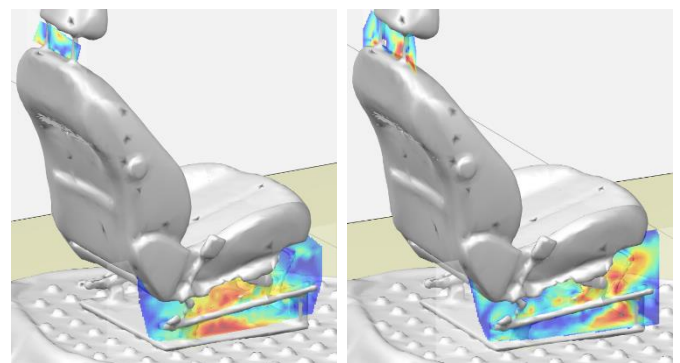


Figure 9. Sound intensity slices in two frequency ranges: 800 Hz to 2 kHz (left) and 2 kHz to 10 kHz (right) with a 15 dB dynamic range.

The represented values correspond to the norms of the 3D intensity vectors. It becomes then clear that the rear part of the seat slide can be associated S&R noise in the 800 Hz to 2 kHz band, whilst the front part of the slider produces most of the acoustic excitation between 2 kHz and 10 kHz.

Active and Reactive Intensity

All results presented above were focused on analyzing the active part of the sound intensity, i.e. the acoustic energy that propagates away from the source towards the far field. However, significant information can also be obtained from evaluating the reactive intensity field. In vibro-acoustic problems comprising coupled mechanical elements, the reactive intensity is mostly related to structure-borne excitation that does not radiate sound efficiently. However, structural vibrations can induce noise problems when the mounting conditions change or additional elements are attached to the excited structure. Figure 10 shows results of active and reactive sound intensity between 20 Hz and 375 Hz. As can be seen, the sources of excitation are different depending on the quantity visualized. The bottom section of the seat is the main noise radiation element whereas the back and headrest are the ones presenting the highest reactive intensity. A possible explanation for this phenomenon is that a high displacement does not necessarily imply sound emission when the radiation impedance of the vibrating surface is low. Therefore, high evanescent excitation can only be observed on the headrest and back seat via reactive intensity.

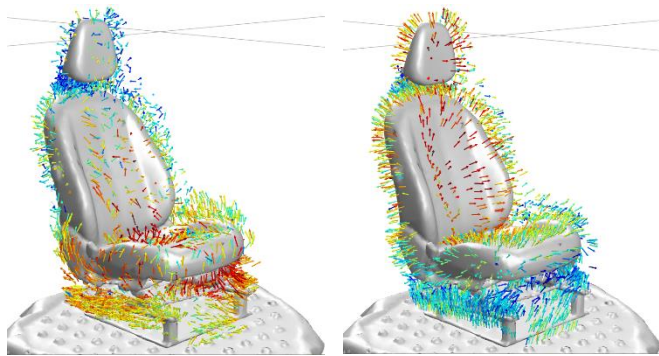


Figure 10. Active (left) and reactive (right) sound intensity between 20 Hz and 375 Hz with a 15 dB dynamic range.

Conclusions

A novel measurement method to perform S&R testing was introduced. Multiple measurements were performed using a production-series vehicle seat mounted on a multi-axial shaker inside a semi-anechoic chamber. The impact of using short excitation signals looped over time to preserve time-stationarity was proven to yield a very similar acoustic output.

It was found that the scanning 3D measurements performed with the Scan&Paint 3D system were effective to localize the main components responsible for the noise radiation (sliders and headrest guides). Several examples with 3D (active and reactive) sound intensity vector maps and 2D slices were provided to visualize the sound fields and assess the location of the noise sources. As shown, the visualization of sound intensity in a 3D space enables to get an intuitive and comprehensive understanding about sound radiation mechanisms as well as the interaction between problematic elements.

In future research, acoustic particle velocity and sound intensity could be used in combination with psychoacoustic analysis and noise source separation in order to objectively predict the annoyance caused by S&R noises.

References

1. Shorter, P.J., Cotoni, V., Chaigne, S., and Langley, R.S. "Predicting the acoustics of squeak and rattle," SAE Technical Paper 2011-01-1585, 2011.
2. Nolan, S.A., and Sammut, J.P., "Automotive squeak and rattle prevention," SAE Technical Paper 921065, 1992.
3. Kavarana, F., and Rediers, B., "Squeak and rattle - state of the art and beyond," SAE Technical Paper 1999-01-1728, 1999.
4. Latorre Iglesias, E., González Figueroa, D., and San Millán Castillo, R., "Comparison between subjective evaluation and psychoacoustic parameters for car steering wheel rattle noise assessment," In Proceedings of Euroregio, 2016.
5. SAE International "J1060: Subjective Rating Scale for Evaluation of Noise and Ride Comfort Characteristics Related to Motor Vehicle Tires," SAE Standard, 2000.
6. Cerrato-Jay, G., Gabiniewicz, J., and Gatt, J., "Automatic detection of buzz, squeak and rattle events," Journal of the Acoustical Society of America 135(4):2297, 2014.
7. Fernandez Comesaña, D., Carrillo Pousa, G., and Tijs, E., "Integration of an End-of-Line System for Vibro-Acoustic Characterization and Fault Detection of Automotive Components Based on Particle Velocity Measurements," SAE Technical Paper 2017-01-1761, 2017.
8. Fernandez Comesaña, D., Steltenpool, S., Korbasiwicz, M., and Tijs, E., "Direct acoustic vector field mapping: new scanning tools for measuring 3D sound intensity in 3D space," In proceedings of Euronoise, pp. 891-895, 2015.
9. Jacobsen, F., and Juhl, P. M., "Fundamentals of general linear acoustics," John Wiley & Sons, 2013.
10. Kinsler, L.E., Frey, A.R., Coppens, A.B., and Sanders J. V., "Fundamentals of acoustics," Wiley, 2000.
11. Fahy, F.J. "Sound Intensity," E&FN Spon, 2nd edition, 1995.
12. Druyvesteyn, W.F., and de Bree, H.-E.. "A new sound intensity probe comparison with the pair of pressure microphones intensity probe," Journal of the Audio Engineering Society 48(1/2):49-56, 2000.
13. Jacobsen, F., and de Bree, H.-E., "A comparison of two different sound intensity measurement principles." Journal of the Acoustical Society of America 118(3): 1510-1517, 2005.
14. Jacobsen, F., and de Bree, H.-E.. "Measurement of sound intensity: p-u probes versus p-p probes," In proceedings of NOVEM, 2005.
15. Occipital, Inc. "The structure sensor", <https://www.structure.io/>, 2008 (accessed 8th December 2019).

Contact Information

Daniel Fernández Comesaña,
CTO at Microflown Technologies.
fernandez@microflown.com
<https://www.microflown.com>

Acknowledgments

The authors would like to thank Laura Rivas López, Manuel Vilas Alonso and Gabriel Brais Martínez Silvosa for their kind support and valuable input during the experimental investigation and subjective evaluation.